

Distribution of valence quarks in hadrons in QCD: theoretical method of solution.

B.L.Ioffe

Institute of Theoretical and Experimental Physics.
B.Cheremuskinskaya 25. 117218 Moscow. Russia

The general method for calculation of valence quark distributions in hadrons at intermediate x is presented. The imaginary part of virtual photon forward scattering amplitude on quark current with hadron quantum number is considered in the case, when initial and final virtualities of the current p_1^2 and p_2^2 are different, negative and large: $|p_1^2|, |p_2^2| \gg R_c^{-2}$, where R_c is confinement radius. The operator product expansion (OPE) in p_1^2, p_2^2 up to dimension 6 operators is performed. Double dispersion representations in p_1^2, p_2^2 of the amplitude in terms of physical states contributions are used. Equalling them to those calculated in QCD by OPE the desired sum rules for quark distributions in mesons are found. The double Borel transformations are applied to the sum rules, killing non-diagonal transition terms, which deteriorated the accuracy in the previous calculations of quark distributions in nucleon. Leading order perturbative corrections are accounted. Valence quark distributions in pion, longitudinally and transversally polarized ρ -mesons and proton are calculated at intermediate x , $0.2 \lesssim x \lesssim 0.7$ and normalization points $Q^2 = 2 - 5 \text{ GeV}^2$ with no fitting parameters. In cases of pion and proton the results are in agreement with found correspondingly from the data on the Drell-Yan process and deep inelastic scattering. Valence quark distributions in transversally and longitudinally polarized ρ -mesons are essentially different one from another and also differ from those in pion.

1. Introduction

Quark and gluon distributions in hadrons are not fully understood in QCD. QCD predicts the evolution of these distributions with Q^2 in accord with the Dokshitzer-Gribov-Lipatov-Altarelli-Parisi (DGLAP) [1]-[3] equations, but not the initial values from which this evolution starts. The standard way of determination of quark and gluon distributions in nucleon is the following [4-8] (for the recent reviews [9]). At some $Q^2 = Q_0^2$ (usually, at low or intermediate $Q^2 \sim 2 - 5 \text{ GeV}^2$) the form of quark (valence and sea) and gluon distributions is assumed and characterized by the number of free parameters. Then, by using DGLAP equations, quark and gluon distributions are calculated at all Q^2 and x and compared with the whole set of the data on deep inelastic lepton-nucleon scattering (sometimes also with prompt photon production, jets at high p_{\perp} etc; for pion – with the data on Drell-Yan process). The best fit for the parameters is found and, therefore, quark and gluon distributions are

defined at all Q^2 , including their initial values $q(Q_0^2, x)$, $g(Q_0^2, x)$. Evidently, such an approach is not completely satisfactory from the theoretical point of view - it would be desirable to determine the initial distribution directly from QCD.

I present you based on QCD method of the calculation of u and d valence quark distributions in hadrons at low $Q^2 \sim 2 - 5 \text{ GeV}^2$ and intermediate x . The idea of the method was suggested in [10] and developed in [11-13]. Recently, the method had been improved and valence quark distributions in pion [14] and transversally and longitudinally polarized ρ -meson [15] had been calculated, what was impossible in the initial version of the method. For valence quark distributions in proton the improved method [16] gave a much better agreement with experiment, than the earlier version [11]. The idea of the approach (in the improved version) is to consider the imaginary part (in s -channel) of a four-point correlator $\Pi(p_1, p_2, q, q')$ corresponding to the forward scattering of two quark currents, one of which has the quantum numbers of hadron of interest and the other is electromagnetic. It is supposed that virtualities of the photon q^2, q'^2 and hadron currents p_1^2, p_2^2 are large and negative $|q^2| = |q'^2| \gg |p_1^2|, |p_2^2| \gg \frac{1}{c^2}$, where c is the confinement radius. It was shown in [11] that in this case the imaginary part in s -channel [$s = (p_1 + q)^2$] of $\Pi(p_1, p_2; q, q')$ is dominated by a small distance contribution at intermediate x . (The standard notation is used: x is the Bjorken scaling variable, $x = -q^2/2\nu$, $\nu = p_1 q$). The proof of this statement, given in [11], is based on the fact that for the imaginary part of the forward scattering amplitude the position of the closest to zero singularity in momentum transfer is determined by the boundary of the Mandelstam spectral function and is given by the equation

$$t_0 = -4 \frac{x}{1-x} p^2 \quad (1)$$

Therefore, if $|p^2|$ is large and x is not small, then even at $t = 0$ (the forward amplitude) the virtualities of intermediate states in t -channel are large enough for OPE to be applicable. So, in the mentioned above domain of q^2, q'^2, p_1^2, p_2^2 and intermediate x $Im\Pi(p, p_2; q, q')$ can be calculated using the perturbation theory and the operator product expansion in both sets of variables $q^2 = q'^2$ and p_1^2, p_2^2 . The approach is inapplicable at small x and x close to 1. This can be understood for physical reasons. In deep inelastic scattering at large $|q^2|$ the main interaction region in spacetime is the light-cone domain and longitudinal distances along the light-cone are proportional to $1/x$ and become large at small x [17,18]. For OPE validity it is necessary for these longitudinal distances along light-cone to be also small, that is not the case at small x . At $1-x \ll 1$ another condition of applicability of the method is violated. The total energy squares $s = Q^2(1/x - 1) + p_1^2$, $Q^2 = -q^2$ is not large at $1-x \ll 1$. Numerically, the typical values to be used below are $Q^2 \sim 5 \text{ GeV}^2$, $p_1^2 \sim -1 \text{ GeV}^2$. Then, even at $x \approx 0.7$, $s \approx 1 \text{ GeV}^2$, i.e., at such x we are in the resonance region. So, one may expect by hand, that our method could work only up to $x \approx 0.7$. The inapplicability of the method at small and large x manifests itself in the blow-up of high order terms of OPE. Moreover, precise limits on the applicability domain in x will be found from the magnitude of the terms.

The further procedure is common for QCD sum rules. On one hand the four-point correlator $\Pi(p_1, p_2; q, q')$ is calculated by perturbation theory and OPE. On the other hand, the double dispersion representation in p_1^2, p_2^2 in terms of physical state contributions is written for the same correlator and the contribution of the lowest state is extracted using the Borl transform. By equating these two expressions the desired quark distribution is found.

. The method

Consider the forward 4-point correlator:

$$\Pi(p_1, p_2; q, q') = -i \int d^4x d^4y d^4z e^{ip_1x+iqy-ip_2z} \times \langle 0 | T \{ \not{j}^h(x), \not{j}^{\text{el}}(y), \not{j}^{\text{el}}(0), \not{j}^h(z) \} | 0 \rangle \quad (2)$$

Here p_1 and p_2 are the initial and final momenta carried by hadronic current \not{j}^h , q and $q' = q + p_1 - p_2$ are the initial and final momenta carried by virtual photons. (Lorentz indices are omitted). It will be very essential for us to consider non-equal p_1, p_2 and treat p_1^2, p_2^2 as two independent variables. However, we may put $q^2 = q'^2 = q^2$ and $t = (p_1 - p_2)^2 = 0$. We are interested in imaginary part of $\Pi(p_1^2, p_2^2, q^2, s)$ in s channel:

$$\text{Im}\Pi(p_1^2, p_2^2, q^2, s) = \frac{1}{2i} \left[\Pi(p_1^2, p_2^2, q^2, s + i\varepsilon) - \Pi(p_1^2, p_2^2, q^2, s - i\varepsilon) \right] \quad (3)$$

In order to construct the representation of $\text{Im}\Pi(p_1^2, p_2^2, q^2, s)$ in terms of contributions of physical states, let us write for $\text{Im}\Pi(p_1^2, p_2^2, q^2, s)$ the double dispersion relation in p_1^2, p_2^2 :

$$\begin{aligned} \text{Im}\Pi(p_1^2, p_2^2, q^2, s) &= a(q^2, s) + \int_0^\infty \frac{\varphi(q^2, s, u)}{u - p_1^2} d^4u + \int_0^\infty \frac{\varphi(q^2, s, u)}{u - p_2^2} d^4u \\ &+ \int_0^\infty \int_0^\infty d^4u_1 d^4u_2 \frac{\rho(q^2, s, u_1, u_2)}{(u_1 - p_1^2)(u_2 - p_2^2)} \end{aligned} \quad (4)$$

The second and the third terms in the right-hand side (rhs) of (4) may be considered as subtraction terms to the last one – the properly double spectral representation. The first term in the rhs of (4) is the subtraction term to the second and third ones. Therefore, (4) has the general form of the double spectral representation with one subtraction in both variables – p_1^2 and p_2^2 . Apply the double Mellin transformation in p_1^2, p_2^2 to (4). This transformation kills the first terms in rhs of (4) and we have

$$\mathcal{B}_{M_1^2} \mathcal{B}_{M_2^2} \text{Im}\Pi(p_1^2, p_2^2, q^2, s) = \int_0^\infty d^4u_1 \int_0^\infty d^4u_2 \rho(q^2, s, u_1, u_2) \exp \left[-\frac{u_1}{M_1^2} - \frac{u_2}{M_2^2} \right] \quad (5)$$

The integration region over u_1, u_2 may be divided into 4 areas as:

- I. $u_1 < s_0; u_2 < s_0$
- II. $u_1 < s_0; u_2 > s_0$
- III. $u_1 > s_0; u_2 < s_0$
- IV. $u_1, u_2 > s_0$

Using the standard QCD sum rule model of hadronic spectrum and the hypothesis of quark-hadron duality, i.e. the model with one low state resonance plus continuum, one may see, that area I corresponds to resonance contribution. Spectral density in this area can be written as

$$\rho(u_1, u_2, x, Q^2) = g_h^2 \cdot 2\pi F_2(x, Q^2) \delta(u_1 - m_h^2) \delta(u_2 - m_h^2), \quad (6)$$

where g_h is defined as

$$\langle 0 | \not{j}_h | \rangle = g_h \quad (7)$$

(For simplicity we consider the case of the Lorentz scalar hadronic current.) If in $Im\Pi(p_1, p_2, q, q')$ the structure, proportional to $P \cdot P$ [$P = (p_1 + p_2) / 2$] is considered, then in the lowest twist approximation $F_2(x, Q^2)$ is the structure function, depending on the Bjorken scaling variable x and weakly on $Q^2 = -q^2$.

In area (IV), where both variables $u_{1,2}$ are far from resonance region, the non-perturbative effects may be neglected, and as usual in sum rules, the spectral function of hadron state is described by the bare loop spectral function ρ^0 in the same region

$$\rho(u_1, u_2, x) = \rho^0(u_1, u_2, x) \quad (8)$$

In areas (II),(III) one of the variables is far from the resonance region, but the other is in the resonance region, and the spectral function in this region is some unknown function $\rho = \psi(u_1, u_2, x)$, which corresponds to transitions like $\rightarrow continuum$. The areas II-III contributions are exponentially suppressed, and, using the standard hypothesis of quark-hadron duality, we may estimate them as a bare loop contribution in the same integration region. Equating physical and QCD representation of Π and taking into account cancellation of appropriate parts in the left and right sides, one can write the following sum rule:

$$Im \Pi_{\text{QCD}}^0 + \text{Power correction} = 2\pi F_2(x, Q^2) g_h^2 e^{-m_h^2(\frac{1}{M_1^2} + \frac{1}{M_2^2})}$$

$$Im \Pi_{\text{QCD}}^0 = \int_0^1 \int_0^1 \rho^0(u_1, u_2, x) e^{-\frac{u_1 + u_2}{2M^2}} \quad (9)$$

It can be shown (see below), that for bare loop diagram $\psi(u_1, u_2, x) \sim \delta(u_1 - u_2)$, and, as a consequence, the areas II and III contributions are zero in our model of hadronic spectrum.

It is worth mentioning that if we would consider the forward scattering amplitude from the beginning, put $p_1 = p_2 = p$ and perform \mathbf{B} or \mathbf{L} transformation in p^2 , then unlike (5), the contributions of the second and third terms in (4) would not vanish. They just correspond to the non-diagonal transition matrix elements and are proportional to

$$\langle 0 | \not{p}^h | * \rangle \frac{1}{p^2 - m_h^{*2}} \langle * | \not{p}^{\text{el}}(x) \not{p}^{\text{el}}(0) | \rangle \frac{1}{p^2 - m_h^2} \langle \not{p}^h | 0 \rangle \quad (10)$$

From decomposition

$$\frac{1}{p^2 - m_h^{*2}} \frac{1}{p^2 - m_h^2} = \frac{1}{m_h^{*2} - m_h^2} \left(\frac{1}{p^2 - m_h^{*2}} - \frac{1}{p^2 - m_h^2} \right) \quad (11)$$

it is clear that in this case (10) may contribute to the second (or third) term in (4) and after \mathbf{B} or \mathbf{L} transformation the contribution of the second term in (11) has the same \mathbf{B} or \mathbf{L} exponent $e^{-m_h^2 = M^2}$ as the lowest resonance contribution. The only difference is in pre-exponential factors: they are $1/M^2$ in front of the resonance term and Const. in front of non-diagonal terms. This difference was used in order to get rid of non-diagonal terms: application of the differential operator $(\partial/\partial(1/M^2))e^{m_h^2 = M^2}$ to the sum rule kills the \mathbf{B} or \mathbf{L} non-suppressed non-diagonal terms, but deteriorates the accuracy and shrinks the applicability domain of the sum rule (particularly, the domain in x , where the sum rule is valid).

3. u -quark distributions in pion

It is enough to find the distribution of valence u -quark in π^+ , since $\bar{c}(x) = u(x)$. The most suitable hadronic current in this case is the axial current

$$j_5 = \bar{u}\gamma_5 c \quad (12)$$

In order to find the u -quark distribution, the electromagnetic current is chosen as u -quark current with the unit charge

$$j^{\text{el}} = \bar{u}\gamma u \quad (13)$$

The bar loop Fig.1 contribution is given by

$$\begin{aligned} \text{Im } \Pi &= - \left\{ \frac{3}{(2\pi)^2} \frac{1}{2} \frac{c^4 k}{k^2} \frac{1}{(k+p_2-p_1)^2} \delta[(q+k)^2] \delta[p_1-k]^2 \right. \\ &\quad \left. \times T_{\bullet} \left\{ \gamma \hat{k} \gamma (\hat{k} + \hat{q}) \gamma (\hat{k} + \hat{p}_2 - \hat{p}_1) \gamma (\hat{k} - \hat{p}_1) \right\} \right\} \quad (14) \end{aligned}$$

It is convenient to introduce

$$P = (p_1 + p_2)/2, \quad \bullet = p_1 - p_2, \quad \bullet^2 = 0 \quad (15)$$

The tensor structure, chosen to construct the sum rule is a structure proportional to $P P P P / \nu$. The reasons are the following. The results of the QCD sum rules calculations are more reliable, if invariant amplitude at kinematical structure with maximal dimension is used. Different $p_1 \neq p_2$ are important only in denominators, where they allow one to separate the terms in dispersion relations. In numerators one may restrict oneself to consideration of terms proportional to 4-vector P and ignore the terms $\sim \bullet$. Then the factor $P P$ provides the contribution of $F_2(x)$ structure function and the factor $P P$ corresponds to contribution of spin zero states. (The factor $1/\nu$ is scaling factor: $w_2 = F_2/\nu$.)

Let us use the notation

$$\Pi = (P P P P / \nu) \Pi(p_1^2, p_2^2, x) + \dots \quad (16)$$

Then $\text{Im} \Pi(p_1^2, p_2^2, x)$ can be calculated from (14) and the result is [14]:

$$\text{Im} \Pi(p_1^2, p_2^2, x) = \frac{3}{\pi} x^2 (1-x) \int_0^\infty \int_0^\infty \frac{\delta(u_1 - u_2)}{(u_1 - p_1^2)(u_2 - p_2^2)} \quad (17)$$

The matrix element of the axial current between vacuum and pion state is well known

$$\langle 0 | j_5 | \pi \rangle = i p f \quad (18)$$

where $f = 131 \text{ Me}^{-1}$. The use of (9), (17), (18) gives the sum rule for valence u -quark distribution in pion in the bar loop approximation [14]:

$$u(x) = \frac{3}{2\pi^2} \frac{M^2}{f^2} x(1-x) (1 - e^{-s_0=M^2}) e^{m_\pi^2 - M^2}, \quad (19)$$

where s_0 is the continuum threshold. In ref.[14] the following corrections to (19) were accounted:

1. Leading order (LO) perturbative corrections, proportional to $\ln(Q^2/\mu^2)$, where μ^2 is the normalization point. In what follows the normalization point will be chosen to be equal to the \mathbf{B} orl parameter $\mu^2 = M^2$.

2. Higher order terms of OPE. Among them, the dimension-4 correction, proportional to gluon condensate $\langle 0 | -\frac{1}{2} G^a G^a | 0 \rangle$ was first accounted, but it was found that its contribution to the sum rule vanishes after doublet reduction. There are two types of vacuum expectation values (v. .v) of dimension 6: one, where only gluonic fields enter:

$$\frac{g_s}{\pi} \alpha_s f^{abc} \langle 0 | G^a G^b G^c | 0 \rangle \quad (20)$$

and the other, proportional to four-quark operators

$$\langle 0 | \bar{\psi} \Gamma \psi \cdot \bar{\psi} \Gamma \psi | 0 \rangle \quad (21)$$

It was shown in [14] that terms of the first type cancel in the sum rule and only terms of the second type survive. For the latter one may use the factorization hypothesis which reduces all the terms of this type to the square of quark condensate.

A remark is in order here. As was mentioned in the Introduction, the present approach is invalid at small and large x . No-loop 4-quark condensate contributions are proportional to $\delta(1-x)$ and cannot be accounted. In the same way, the diagrams, which can be considered as radiative corrections to those, proportional to $\delta(1-x)$, must be also omitted.

All dimension-6 power corrections to the sum rule were calculated in refs. 14,15 and the final result is given by:

$$\begin{aligned} xu(x) = & \frac{3}{2\pi^2} \frac{M^2 e^{m_\pi^2 = M^2}}{f^2} x^2 (1-x) \left[\left(1 + \left(\frac{a_s(M^2) \cdot \ln(Q_0^2/M^2)}{3\pi} \right) \right) \right. \\ & \times \left(\frac{1 + 4x \ln(1-x)}{x} - \frac{2(1-2x) \ln x}{1-x} \right) \cdot (1 - e^{-s_0 = M^2}) \\ & \left. - \frac{4\pi \alpha_s(M^2) \cdot 4\pi \alpha_s a^2}{(2\pi)^4 \cdot 3^7 \cdot 2^6 \cdot M^6} \cdot \frac{\omega(x)}{x^3(1-x)^3} \right], \quad (22) \end{aligned}$$

where $\omega(x)$ is 4-order polynomial in x , (for its explicit form see [14]),

$$a = -(2\pi)^2 \langle 0 | \bar{\psi} \psi | 0 \rangle \quad (23)$$

$u(x)$ may be used as an initial condition at $Q^2 = Q_0^2$ for solution of QCD evolution equations (DGLAP equations).

In numerical calculations we choose: the effective LO QCD parameter $\Lambda_{\text{QCD}}^{\text{LO}} = 250 \text{ MeV}$, $Q_0^2 = 2 \text{ GeV}^2$, $\alpha_s a^2 (1 \text{ GeV}^2) = 0.34 \text{ GeV}^6$. The value of the latter is taken from the recent best fit of hadronic τ -decay data [19] and corresponds to $\alpha_s \langle \bar{\psi} \psi \rangle^2 = (2.2 \cdot 0.7) \cdot 10^{-4} \text{ GeV}^6$. The continuum threshold was varied in the interval $0.8 < s_0 < 1.2 \text{ GeV}^2$ and it was found, that the results only slightly depend on it. The analysis of the sum rule (22) shows, that it is fulfilled in the region $0.15 < x < 0.7$; the power corrections are less than 30% and the continuum contribution is small ($< 25\%$). The stability in the \mathbf{B} orl mass parameter M^2 depends in the region $0.4 \text{ GeV}^2 < M^2 < 0.6 \text{ GeV}^2$ is good. The result of our calculation of valence distribution in pion $xu(x, Q_0^2)$ is shown in Fig.2.

Suppos , that at small $x \lesssim 0.15$ $u(x) \sim 1/\sqrt{x}$ according to Regg behaviour and at larg $x \gtrsim 0.7$ $u(x) \sim (1-x)^2$ according to quark counting rules. Then, matching these functions with (22), one may find the numerical values of the first and second moments of u -quark distribution

$$\mathcal{M}_1 = \int_0^1 u(x) dx \approx 1.1 \quad (24)$$

$$\mathcal{M}_2 = \int_0^1 xu(x) dx \approx 0.24 \quad (25)$$

\mathcal{M}_1 has the meaning of the number of u -quarks in π^+ and should be $\mathcal{M} = 1$. The deviation of (24) from 1 characterizes the accuracy of our calculation. \mathcal{M}_2 has the meaning of the part of pion momentum carried by valence u -quark. Therefore, valence u and \bar{d} quarks are carrying about 40% of the total momentum. In Fig.2 are plotted also the valence u -quark distribution found in [4b] by fitting the data on production of $\mu^+\mu^-$ and e^+e^- pairs in pion-nucleon collisions (Drill-Yan process).

4. ~~quark distribution in ρ -meson~~

The choice of hadronic current is evident

$$j = \bar{u}\gamma_5 \quad (26)$$

The matrix element $\langle \rho^+ | j | 0 \rangle$ is given by

$$\langle \rho^+ | j | 0 \rangle = \frac{m^2}{g} e \quad (27)$$

where m is the ρ -meson mass, g is the $\rho - \gamma$ coupling constant, $g^2/4\pi = 1.27$, e is the ρ -meson polarization vector. Consider separately u -quark distributions in longitudinally and transversally polarized ρ -mesons. It was shown in [15], that for determination of u -quark distribution in longitudinal ρ -meson the most suitable tensor structure is that, proportional to $P P P P$, while u -quark distribution in transversal ρ can be found by considering the invariant function at the structure $-P P \delta$. In case of longitudinal ρ -meson the tensor structure, which is separated is the same, as in the case of pion. Since at $m_q = 0$ bar loop contributions for vector and axial hadronic currents are equal, the only difference from the pion case is in the normalization. It can be shown, that u -quark distribution in longitudinal ρ -meson can be found from (22) by substitutions $m \rightarrow m$, $f \rightarrow m/g$ and therefore

$$xu(x) = \frac{f^2}{m^2} g^2 e^{(m_\rho^2 - m_\pi^2) = M^2} xu(x), \quad (28)$$

where $xu(x)$ is given by (22). (The numerical values of M^2 and s_0 differ in the cases of pion and longitudinal ρ -meson). After separation of the invariant function at the structure $P P \delta$ in box diagram we find u -quark distribution in transversally polarized ρ -meson in bar loop approximation:

$$u^T(x)_0 = 3 \left[\frac{1}{2} - x(1-x) \right] \equiv \frac{3}{2} \varphi_0(x) \quad (29)$$

$u^\top(x)_0$ has a minimum at $x = \frac{1}{2}$, unlike $u(x)_0$ and $u^\perp(x)_0$. Another essential difference in comparison with pion and longitudinal ρ arises due to the fact that gluon condensate and $\langle G^3 \rangle$ operator contributions are nonvanishing in the sum rule for $u^\top(x)$.

Valence u -quark distribution in transversally polarized ρ -meson is given by

$$\begin{aligned}
xu^\top(x) = & \frac{3}{8\pi^2} g^2 e^{m_\rho^2 = M^2} \frac{M^4}{m^4} x \left\{ \varphi_0(x) E_1\left(\frac{s_0}{M^2}\right) \left[1 + \frac{1}{3\pi} \ln\left(\frac{Q_0^2}{M^2}\right) \alpha_s(M^2) \left(\frac{4x-1}{\varphi_0(x)} + \right. \right. \right. \\
& \left. \left. \left. + 4\ln(1-x) - \frac{2(1-2x+4x^2)\ln x}{\varphi_0(x)} \right) \right] - \frac{\pi^2}{6} \frac{\langle 0 | (\alpha_s/\pi) G^2 | 0 \rangle}{M^4 x^2} \right. \\
& \left. + \frac{1}{2^8 \cdot 3^5 M^6 x^3 (1-x)^3} \langle 0 | g^3 f^{abc} G^a G^b G^c | 0 \rangle \xi(x) \right. \\
& \left. + \frac{\alpha_s(M^2) (\alpha_s a^2)}{2^5 \cdot 3^8 \pi^2 M^6 x^3 (1-x)^3} \chi(x) \right\} \quad (30)
\end{aligned}$$

where $\xi(x)$ and $\chi(x)$ are polynomials in x [15]. In numerical calculations the values of parameters were chosen: $M^2 = 1 \text{ GeV}^2$ (this value is in the middle of stability interval in M^2), $s_0 = 1.5 \text{ GeV}^2$, $Q_0^2 = 4 \text{ GeV}^2$, $\langle 0 | (\alpha_s/\pi) G^2 | 0 \rangle = 0.006 \text{ GeV}^2$ [20], $\langle G^3 \rangle$ vacuum expectation value was estimated according to instanton model [21]. The effective instanton radius, was taken to be equal $\rho_c = 0.5 \text{ fm}$. The other parameters are the same as in calculation of $xu(x)$. On Fig.3 are plotted $u^\perp(x)$, $u^\top(x)$ and, for comparison, $u(x)$. As is seen from the Figure, the shape of $u^\top(x)$ is quite different from $u(x)$ and $u^\perp(x)$ and indicates, that perhaps, $u^\top(x)$ has two humps. $u^\perp(x)$ also has an interesting feature: the condensate moment of u -quark distribution is equal to 0.4. It means, that the part of ρ^\perp momenta, carried by valence u and \bar{u} quarks comprises 80% and for gluons and sea quarks is left about 20% only – a very unusual situation!

The main physical conclusion is: the quark distributions in pion and ρ -meson have not much in common. The specific properties of pion, as a Goldstone boson manifest themselves in different quark distributions in comparison with ρ .

5. Quark distributions in proton

Consider the 4-current correlator which corresponds to the virtual photon scattering on the quark current with quantum number of proton:

$$T(p_1, p_2, q, q') = -i \int d^4x d^4y d^4z \cdot e^{i(p_1 x + q y - p_2 z)} \cdot \langle 0 | T \{ \mathcal{J}(x), \mathcal{J}^{u(d)}(y), \mathcal{J}^{u(d)}(0), \bar{\mathcal{J}}(z) \} | 0 \rangle, \quad (31)$$

where $\mathcal{J}(x)$ is the three-quark current $\mathcal{J}(x) = \varepsilon^{abc} (u^a C \gamma u^b) \gamma_5 \gamma^c \bar{\mathcal{J}}^c$ [22], $\mathcal{J}^u = \bar{u} \gamma u$, $\mathcal{J}^d = \bar{d} \gamma d$. As was shown in [11] and generalized to non equal p_1, p_2 in [16] the sum rules should be written for invariant amplitude at the structure $\hat{p} p p$ (it what follows it will be denoted by ImT/ν). The bar loop diagram is shown on Fig.4. The result of its calculation after the double Fourier transformation are the same as in the case for equal $p_1 = p_2$ [11]:

$$ImT_{u(d)}^0 = \varphi_0^{u(d)}(x) \frac{M^2}{32\pi^3} E_2(s_0/M^2) \quad (32)$$

where

$$\varphi_0^u(x) = x(1-x)^2(1+8x), \quad \varphi_0^d(x) = x(1-x)^2(1-2x), \quad (33)$$

s_0 is the continuum threshold

$$E_2(z) = 1 - (1 + z + z^2/2)e^{-z} \quad (34)$$

The sum rules for u and \bar{c} -quark distributions $q(x)^{u(d)}$ in bar loop approximation are:

$$xq(x)_0^{u(d)} = \frac{2M^6 e^{m^2=M^2}}{\bar{\lambda}_N^2} \varphi_0^{u(d)}(x) \cdot E_2\left(\frac{s_0}{M^2}\right) \quad (35)$$

Here λ_N is the coupling constant of proton with the current $\langle 0 | \bar{\psi} | p, \psi \rangle = \lambda_N v^r(p)$, $\bar{\lambda}_N^2 = 32\pi^4 \lambda_N^2$. The first and second moments of quark distributions, with account of proton mass sum rule in the same approximation, coincide with quark model results, as it should be. QCD evolution was accounted as leading order (LO) correction to bar loop formula (see [16]). In OPE the contributions of $\bar{c} = 4$ operator (gluon condensate) and $\bar{c} = 6$ operator (α_s times quark condensate squared) was calculated. I present here the results as the ratio to bar loop contributions:

$$\frac{u(x)_{\langle G^2 \rangle}}{u_0(x)} = \frac{\langle (\alpha_s/\pi) G^2 \rangle}{M^4} \cdot \frac{\pi^2}{12} \frac{(11 + 4x - 31x^2)}{x(1-x)^2(1+8x)} \cdot (1 - e^{-s_0/M^2}) / E_2\left(\frac{s_0}{M^2}\right) \quad (36)$$

$$\frac{\bar{c}(x)_{\langle G^2 \rangle}}{\bar{c}_0(x)} = -\frac{\langle (\alpha_s/\pi) G^2 \rangle}{M^4} \frac{\pi^2}{6} \frac{(1 - 2x^2)}{x^2(1-x)^2(1+2x)} (1 - e^{-s_0/M^2}) / E_2\left(\frac{s_0}{M^2}\right) \quad (37)$$

$$\frac{u(x)_{s_0^{-1/2}}}{u_0(x)} = \frac{\alpha_s a^2 (215 - 867x + 172x^2 + 288(1-x)\ln 2)}{M^6 \cdot 81\pi \cdot 8x(1-x)^3(1+8x)} \frac{1}{E_2(s_0/M^2)} \quad (38)$$

$$\frac{\bar{c}(x)_{s_0^{-1/2}}}{\bar{c}_0(x)} = -\frac{\alpha_s a^2 (19 - 43x + 36x^2)}{M^6 81\pi x(1-x)^3(1+8x)} \frac{1}{E_2(s_0/M^2)} \quad (39)$$

On Fig. 5 are plotted the obtained u and \bar{c} -quark distributions at $Q_0^2 = 5 \text{ GeV}^2$ in comparison with those found in [4a] from the data on deep inelastic lepton-nucleon scattering. The same values of QCD parameters (condensates) were taken as in cases of quark distributions in π and ρ . The form factor M^2 was chosen in the middle of stability interval, $M^2 = 1.1 \text{ GeV}^2$.

The theoretical analysis of the obtained valence quark distributions at $Q^2 = 5 \text{ GeV}^2$ shows that u -quark distribution is reliable at $0.15 < x < 0.65$, its accuracy is about 25% in the middle of this interval and decreases to 50% at the ends of interval; \bar{c} -quark distribution is reliable at $0.25 < x < 0.55$ with an accuracy of about 30% in the middle and is given by a factor of 2 at the ends of interval. In the limit of these accuracies the theoretically calculated valence quark distributions are in agreement with those found from deep inelastic scattering and other hard process data.

This research described in this publication was made possible in part by Award No. RP2-2247 of the US Civilian and Developmental Foundation for the Independent States of Former Soviet Union (CRDF), by INTAS Grant 2000, Project 587 and by the Russian Foundation of Basic Research, Grant No. 00-02-17808.

References

- [1] V.N.Gribov and L.N.Lipatov, *Sov. J. Nucl. Phys.* **15** (1972) 438.
- [2] Yu.L.Dokshitz, *Sov. Phys. JETP*, **46** (1977) 641.
- [3] G.Altarelli and G.Parisi, *Nucl. Phys.* **B126** (1977) 298.
- [4] M.Glück, E.Raya and A.Vogt, *J. Phys.* **C53** (1992): a) p.127; b) p.651.
- [5] H.L.Lai et al. (CTEQ Collab.) *Eur. Phys. J.* **C12** (2000) 375.
- [6] A.D.Martin, R.G.Roberts, W. Stirling and R.S.Thorn, *Eur. Phys. J.* **C.4** (1998) 463.
- [7] M.Glück, E.Raya and A.Vogt, *Eur. Phys. J.* **C5** (1998) 461.
- [8] A.M.Cooper-Sarkar, R.C.E.Davies and A.D. Roach, *Int. J. Mod. Phys.* **A13** (1998) 3385.
- [9] Wu-Ki Tung, At the Frontiers of Particle Physics, in: Handbook of QCD, Boris Ioff Festschrift, ed. by M. Shifman, World Sci. 2001, v.2, p.887.
- [10] B.L.Ioff, *Pis'ma v Zh. Eksp. Fiz.* **42** (1985) 266, [*JETP Lett* **42** (1985) 327].
- [11] V.M. Belyaev and B.L.Ioff, *Nucl. Phys.* **B310** (1988) 310.
- [12] A.S.Gorsky, B.L.Ioff, A.Yu.Khodjamirian and A.G.Oganessian, *J. Phys.* **C44** (1989) 523.
- [13] B.L.Ioff and A.Yu.Khodjamirian, *Phys. Rev.* **D51** (1995) 3373.
- [14] B.L.Ioff and A.Oganessian, *Eur. Phys. J.* **C13** (2000) 485.
- [15] B.L.Ioff and A.G.Oganessian, *Phys. Rev.* **D63** (2001), 096006.
- [16] B.L.Ioff and A.Oganessian, hep-ph/0208192.
- [17] V.N.Gribov, B.L.Ioff and I.Ya.Pomeranchuk, *Yad. Fiz.* **2** (1965) 768. [*Sov. J. Nucl. Phys.* **2** (1966) 549].
- [18] B.L.Ioff, *Phys. Lett.* **30 B** (1969) 123.
- [19] B.L.Ioff and K.N. Kobayashi, *Nucl. Phys.* **A687** (2001) 437.
- [20] B.V.Gshkenberg in, B.L.Ioff and K.N. Kobayashi, *Phys. Rev.* **D64** (2001) 093009.
- [21] V.A.Novikov, M.A. Shifman, A.I.Vainshtein and V.I. Zakharov, *Phys. Lett.* **B86** (1979) 347.
- [22] B.L.Ioff, *Nucl. Phys.* **188** (1981) 317.

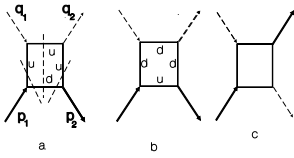


Figure 1: Diagrams, corresponding to the unit operator contribution. Dashed lines with arrows correspond to the photon, thick solid - to pion or rho current.

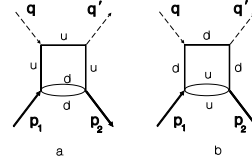


Figure 4: Quark loop diagram in case of proton.

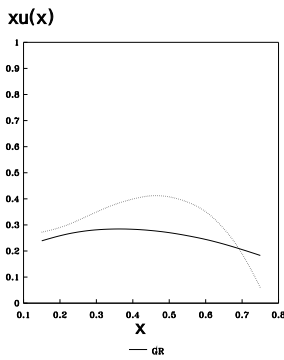


Figure 2: Quark distribution function in pion (dashed line) and the fit from [4b] - solid line.

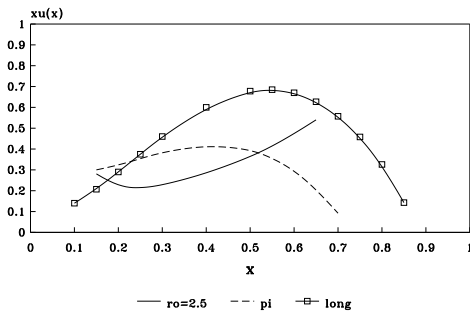


Figure 3: Quark distributions in longitudinal ρ , (solid line with squares), transversal ρ (solid line) and pion (dashed line)

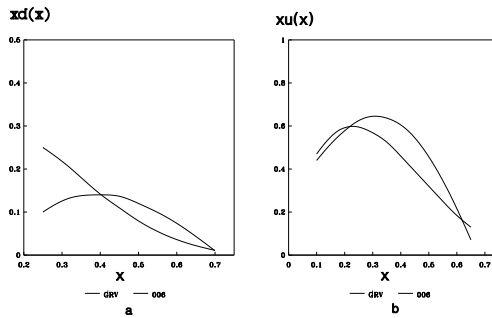


Figure 5: Valence u - and d -quark distributions in proton (dashed lines) in comparison with the fit [4a] of d/p in elastic scattering data (solid lines)